

EFFECT OF CELL COMPOSITION ON INTERNAL RESISTANCE ON OPEN CIRCUIT VOLTAGE AND SHORT CURRENT DENSITY OF A FABRICATED TITANIUM DIOXIDE CELL

David Njoroge Kimemia

ABSTRACT

This paper is a product of a research aimed at developing a solar energy powered titanium dioxide solar cell. The experimental design involved preparation of various ratios of titanium dioxide: graphite /iodine/KI mixtures in each respective layer. Optimization was carried out by varying the mass of the constituents of each layer while maintaining the others constant to obtain the highest current-voltage outputs. The study investigated the effect of the thickness of TiO₂ (the photo active layer) and the electronegative material layers on current-voltage output of the fabricated solar cell. The optimum electricity generation was observed at the ratio of TiO₂/ C_x: I₂: KI as 0.4: 0.3: 0.17: 0.01 g respectively. In conclusion, the results obtained on optimization of a blank cell, the open circuit voltage (V_{OC}) and short circuit current density (J_{SC}) of 0.083 V and 0.33μA were respectively obtained. These values were low confirming that a conducting medium was necessary for the migration of the generated electrons. The research generally recommends that there is need to employ improved technology to reduce presence of air packets which creates air gaps.

Keywords: Cell Composition, Internal Resistance, V_{OC}, J_{SC}

INTRODUCTION

Energy is recognized universally as one of the most fundamental inputs for social and economic development. Modern consumption patterns and energy production contribute significantly to climate change and air pollution. Continued reductions in air pollution and greenhouse gas (GHG) emissions would be essential, as they pose serious threats to both people's health and the environment across the world (IPCC, 2006). In the recent past, the use of renewable energy as an alternative source of energy has increased considerably. This study embarked on solar energy because solar cells manufacturing technology is becoming more reliable and economical. The feasibility of photovoltaic solar energy as an alternative source of energy has become real. However solar pv systems are still compounded with low efficiencies and their dependency on weather conditions still offer room for improvement of the technology to extract higher outputs for different environmental conditions. Therefore, the current study proposes a low cost method of fabricating a renewable source of energy void of greenhouse gas (GHG) emissions.

Air pollution and climate change influence each other through complex interactions in the atmosphere. High levels of GHGs alter the energy balance between the atmosphere and the Earth's surface, which lead to temperature changes that change the chemical composition of the atmosphere. This temperature results to reduced water reservoir on the earth surface which in turn leads to reduced amount of hydro electric energy. There are technological solutions that address concerns of switching off from fossil fuels to renewable forms of energy that cuts down on air pollution emissions (Ferguson *et al.*, 2000). The current study has established a photo cell which will reduce use of fossil fuels and in turn reduce on air pollution and climate change.

The photo cell will be cost effective and environmental friendly by using titanium dioxide in its solid form. Fungo (2007) noted that titanium dioxide has widely been used as white pigment because of its brightness and high refractive index. Sellappan (2013) noted that TiO₂ has ability of generating electrons and holes in the presence of light. When TiO₂ is illuminated with UV radiation, electrons on the surface are activated and fly off leaving electron-deficient holes (Ohama & Van Gemert, 2011) as shown in the equation below.



These discharged electrons have the ability to migrate in a specified direction depending on the nature of the material leading to some conductivity. The conductivity can be improved by adding 'doping with' trace amounts of elements that effectively add or remove electrons from the light illuminated titanium dioxide. Electrons from TiO₂ are excited by UV solar radiation with a wavelength domain of 10nm to 400nm. As a result, the photo electron generation and subsequent conduction of electricity needs to be studied. It can be a preferred semiconductor photo catalytic material due to its non-toxicity, chemical inertness, and stability over a wide pH range under irradiation condition and its relatively favourable disposition of band edges. Microcrystalline TiO₂ powders are also widely employed in the field of heterogeneous catalysis as active component as well as catalyst support (Fungo, 2007).

After considering the utility of titanium dioxide as a photo catalyst and its subsequent application in oxidation of various species, this study has exploited the photo generation of electrons and holes on approaches such as generation of electricity by this material in its solid form upon illumination with a suitable radiation of wavelength domain 10nm to 400nm.

MATERIALS AND METHODS

The study adopted an experimental research design to investigate the performance of the fabricated solar cell. It was done by first obtaining the optimal values of the parameters under investigation. The best parameters were obtained by establishing the optimal values of each material constituent of the cell. These were TiO₂, which was the photoactive material, the graphite which was the conducting medium and the Iodine/Iodide mixture which replenished the electrons conducted away after photo excitation. This process employed varying the weights of the component parts, and finally characterization of the fabricated solar cells under constant radiation intensity in clear daylight.

In the study, the following assumptions were made: The solar radiation was assumed to be constant at 100 mW/cm² irradiance (Hagfeldt *et al.*, 2010); the solar density on the solar cell was assumed to be uniform, and the voltage drop in the digital meter leads was assumed to be negligible. All reagents were of analytical grade and were sourced from Sigma Aldrich. The titanium dioxide (TiO₂), iodine (I₂), potassium iodide (KI) and graphite (C_X) in their powder form were used.

To fabricate the solar cell, different mass ratios of graphite (C_X) powder, titanium dioxide (TiO₂) powder, potassium iodide (KI) and iodine (I₂) were mixed and compressed to form a Solar Cell. Figure 1 below shows the schematic presentation of the fabricated cell.

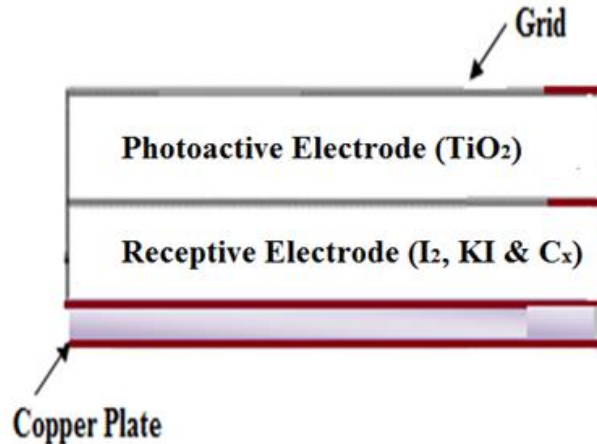


Figure 1: Schematic presentation of the fabricated solar cell

To provide the required dimensions, a copper plate was cut into 2.5 cm by 2.5 cm by the use of metal plate shears. An active cell of \varnothing 1.3 cm ($A=1.327 \text{ cm}^2$) was prepared, laid on the copper plate and covered with a transparent raisin as a copper conductor in contact with the upper electrode was drawn through the raisin for external connection.

The first cell electrode was made by placing the photo active measured sample separately in a circular dice and compressed thoroughly. The second electrode was made by disposing the mixtures of mass ratios of (graphite: iodine: I₂/KI) over the initial layer and the pressing procedure followed. The resultant was a circular pellet which served as the photo active cell. I-V characteristics of each of the resulting cells were monitored. The photo active (cathode) was prepared by varying masses of powdered TiO₂ ranging from (0.2-1) g. These masses were inserted in a moulding dice and pressed into a disc form with a diameter of 1.3 cm to form a circular pellet.

The receptive layer (anode) was prepared by varying masses of finely divided mixtures of mass ratios (graphite: I₂: I₂/KI) ranging from (0.1: 0.1: 0.01) g to (0.6: 0.3: 0.01) g. These mixtures of mass ratios were then inserted in a moulding dice and pressed into a disc form with a diameter of 1.3 cm to form a circular pellet similar in size to the photoactive layer. The receptive layer (anode) was then placed on photo active (cathode) and pressed further to form a complete assembly of the solar cell. External conductors were then connected to the cell for I-V characterization. Figure 2 shows the schematic cell presentation of the solar cell.

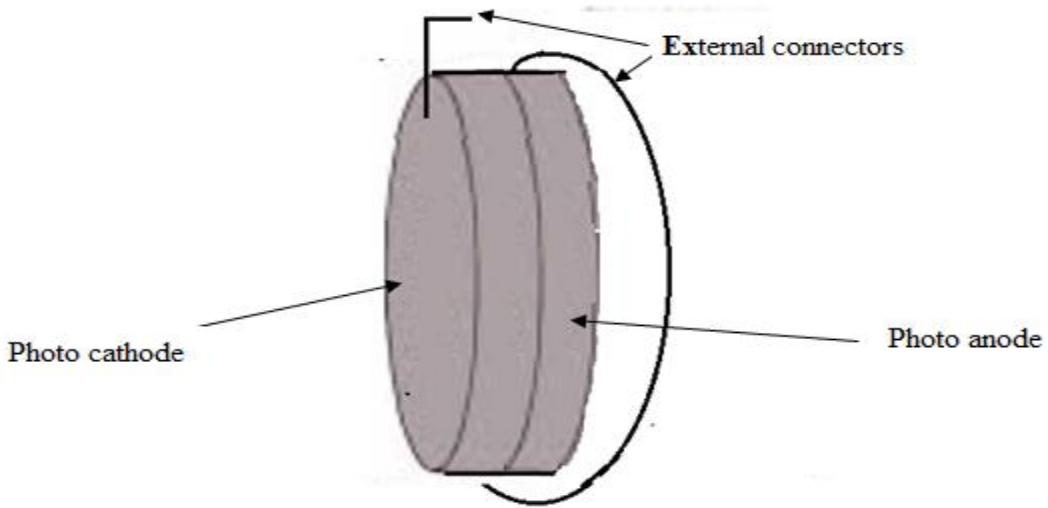


Figure 2: Photo voltaic cell scheme

The optimum I-V characteristics were established using the circuit diagram of Figure 3.

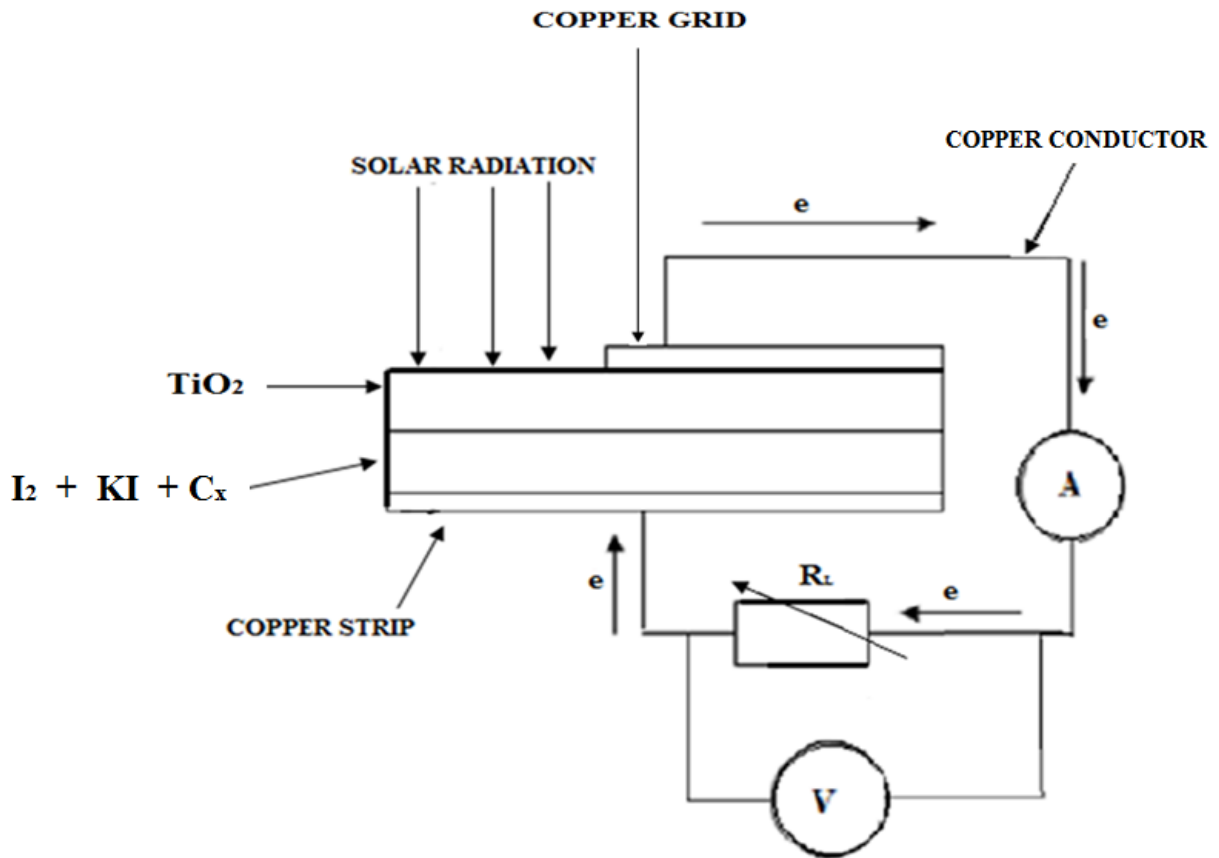


Figure 3: Assembly of the circuit diagram for the I-V characterization

A high resolution micro-Ammeter (0-100 μA) was connected in series with the fabricated Solar cell to measure the current density output (J_{MP}) resulting from the generated charge carriers which migrated from the photo active cathode layer of the cell through external conductors and back to the cell through the anode. A high resolution galvanometer (0-250 mV) was connected in parallel with the arrangement of the \varnothing 1.3 cm ($A=1.327 \text{ cm}^2$) active solar cell and the micro-Ammeter (0-100 μA) to measure the resulting open circuit voltage (V_{OC}) at the output terminals.

A high resolution graduated variable resistor (Ohmmeter) (0-34 Ω) was connected in series with the micro-Ammeter (μA) and in parallel with the galvanometer (0-250 mV). The variable resistor served the purpose of an external load and the ratio of the generated potential (V_{MP}) to the measured resistance at any particular instant, confirmed the amount of the current density (J_{MP}) through the external circuit and this was recorded to determine the maximum power (P_{MAX}) of the solar cell. The short circuit current density ($J_{\text{SC}}/\text{cm}^2$) values were determined at zero applied voltage and the open circuit voltage (V_{OC}) values were determined at zero current under solar radiation. The current generated against their corresponding potential for various cells were collected and tabulated. The voltage output for maximum power output (P_{MAX}) were taken at 5 minutes intervals and tabulated for analysis.

The fabricated solar cell parameters were calculated using equations as applied by Adegbenro (2016) while calculating parameters of different shapes and states of solar cells. In his study, the cells were in 1cm^2 squared blocks while the cell in this study had a diameter of (\varnothing) 1.3 cm giving an area (A) of 1.327 cm^2 :

$$V_{\text{MP}} = \frac{V_{\text{MAX}}}{A} (\text{mV cm}^{-2}) \quad (1)$$

$$J_{\text{MP}} = \frac{I_{\text{MAX}}}{A} (\mu\text{A cm}^{-2}) \quad (2)$$

$$P_{\text{MAX}} = V_{\text{MP}} \times J_{\text{MAX}} \quad (3)$$

$$J_{\text{SC}} = \frac{I_{\text{SC}}}{A} (\mu\text{A cm}^{-2}) \quad (4)$$

$$V_{\text{OC}}/\text{cm}^2 = \frac{V_{\text{OC}}}{A} (\text{mV/ cm}^2) \quad (5)$$

$$P_{\text{T}} = V_{\text{OC}}/\text{cm}^2 \times J_{\text{SC}}/\text{cm}^2 \quad (6)$$

$$\text{Fill Factor(FF)} = \frac{J_{\text{MP}} V_{\text{MP}}}{J_{\text{SC}} V_{\text{OC}}} \quad (7)$$

$$\text{Shunt Resistance}(R_{\text{SH}}) = \frac{\Delta Y}{\Delta X} \quad (8)$$

$$\text{Series Resistance}(R_{\text{S}}) = \frac{\Delta X}{\Delta Y} \quad (9)$$

$$\text{Efficiency } \eta = \frac{J_{\text{SC}} \times \text{FF} \times V_{\text{OC}}}{p_{\text{in}} \times A} \quad (10)$$

'A' is the photoactive area of the cell; $A= 1.327 \text{ cm}^2$. In the study, the parameters were obtained by adopting expression 1-10 as applied by Adegbenro (2016) when he characterized different shapes and states of solar cells to obtain their parameter values.

Jain (2013) defines the open circuit voltage (V_{OC}) is the voltage delivered by the solar cell when the electrodes are isolated and no current is sourced under infinite load resistance. This voltage represents the maximum potential energy stored to initiate the flow of electrons which are yet to be dissipated. Jain also notes that the voltage of a unit area (V_{OC}/cm^2) delivered by a solar cell when the electrodes are isolated represents the maximum potential energy stored to initiate the flow of electrons which are yet to be dissipated.

RESULTS AND DISCUSSION

The optimal values were obtained by varying the composition of one constituent material while maintaining the others constant and monitored the I-V characteristics. The effect of thickness of the optimized cell composition was also studied.

Effect of the cell composition on the internal resistance on V_{OC} and J_{SC}

Analysis of cell S¹

The effect of resistance of cell S¹ whose composition of TiO₂: graphite: I₂ were investigated in the mass ratio (0.7: 0.28: 0.28) as recorded in Table 1.

| Table 1: Composition materials of cell S¹ | | | |
|---|-----------|-----------------|----------------------|
| Mass (g) | | | |
| TiO₂ | KI | Graphite | I₂ |
| 0.7 | 0.01 | 0.28 | 0.28 |

The I-V characteristics obtained from the cell S¹ are as shown in Table 2.

Table 2: Generated potential against current density of solar cell S¹

| Output cell parameters | |
|-------------------------------|--|
| Voltage (V) | Current (J_{sc} (μAcm^{-2})) |
| 0 | 0.05 |
| 0.099 | 0.04 |
| 0.157 | 0.039 |
| 0.199 | 0.036 |
| 0.205 | 0.028 |
| 0.230 | 0.018 |
| 0.238 | 0.014 |
| 0.248 | 0.001 |

From the information shown in Table 2, a graphical presentation of potentials against the current density was made as shown in Figure 1.

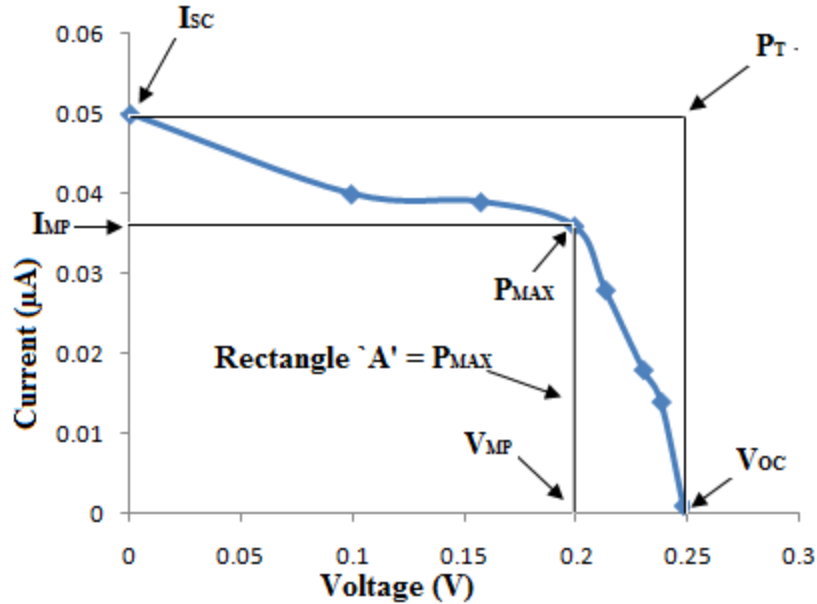


Figure 1: I-V characteristics of cell S¹

It is observed that the mass ratios (0.7: 0.28: 0.28) of TiO₂: graphite: I₂ affected conductivity as a smooth hyperbola was not observed. Figure 1 shows that the current density changes from 0.05 μAcm^{-2} to 0.039 $\mu\text{A cm}^{-2}$ as the potential varied from 0 V to 0.099 V. The curve then assumes almost a constant profile at a potential of 0.099 V to 0.205 V after which there was a steep decrease in current from 0.027 μAcm^{-2} to 0.001 μAcm^{-2} .

The constituent components and the capacitance resulting from the dielectrix was thought to add up to the opposition offered to the flow of the charge carriers as they cross from the photo active layer to the receptive electrode. Similar findings were reported by Imran (2013). According to Yordanov (2012) the departure from the smooth curve was contributed by the parasitic internal resistance.

Low conductivity was also thought to create substitute paths for the generated current which affected negatively on the fill factor and the power output of the solar cell Yordanov (2012). The departure from the smooth curve between a potential of 0 V to 0.099 V can be attributed to internal resistance. Series resistance offers opposition to the flow of the generated current (Piliougineet *al.*, 2011). The sharp decrease in current between a potential of 0.205 V and 0.25 V can be attributed to the effect of series resistance which was found to be 8.65 Ω . The two regions between a potential of 0 mV to 0.25 V indicate the presence of non-ideal carrier recombination losses. This suggested that fewer charge carriers were generated after irradiation. A good solar cell should exhibit low series resistance and low shunt resistance (King *et al.*, 1997).

From the result of Figure 1, an irregular parabolic curve was obtained as opposed to an ideal curve. As a result, the cell could only generate a maximum voltage of 0.248 V/cm² and a maximum current density of 0.05 $\mu\text{A/cm}^2$. The mass of graphite was reduced to 0.28 g and it was also thought to be inadequate to offer a suitable migration medium for the charge carriers. Similar findings were reported by (Renu *et al.*, 2012). The charge carriers were thought to encounter higher series resistance (Rs) as they migrated to the external circuit and hence that

being the reason for the characteristic curve diverting from the normal I-V (Renu *et al.*, 2012). Further experiments were carried out with cells fabricated from different ratios of constituents as discussed in the next section.

Analysis of cell T¹

The effect of resistance of cell T¹ whose composition of TiO₂: graphite: I₂ was investigated in the mass ratios of (0.7: 0.5: 0.4) as presented in Table 3.

Table 3: Composition materials of cell T¹

| T ¹ | Mass (g) | | | |
|----------------|------------------|------|----------|----------------|
| | TiO ₂ | KI | Graphite | I ₂ |
| | 0.7 | 0.01 | 0.5 | 0.4 |

The respective current density corresponding to each value of potential difference was recorded as shown in Table 4.

Table 4: Generated potential against current density of the optimized solar cell T¹

| Output cell parameters | |
|------------------------|--------------------------------|
| Voltage (V) | Current (JμAcm ⁻²) |
| 0 | 0.048 |
| 0.087 | 0.03 |
| 0.146 | 0.033 |
| 0.188 | 0.036 |
| 0.206 | 0.031 |
| 0.221 | 0.028 |
| 0.246 | 0.026 |
| 0.259 | 0.001 |

The cell T¹ was fabricated from the (0.7: 0.5: 0.4) of TiO₂: graphite: I₂. From the graphical representation of potentials against the current density was made as shown in Figure 2.

composition mass ratios (0.7: 0.5: 0.4) of TiO₂: graphite: I₂. From the information recorded in Table 4, a

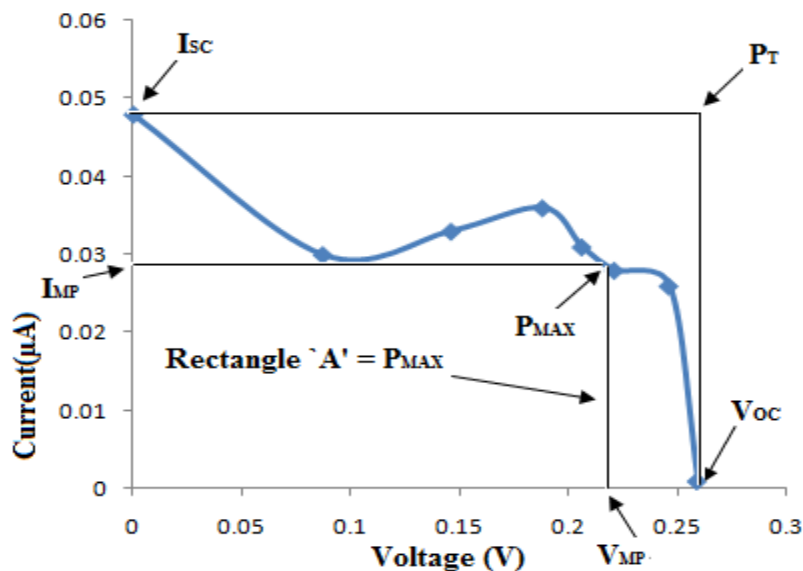


Figure 2: I-V characteristics of cell T¹

The profile of Figure 2 shows a gradual decrease in current from $0.048 \mu\text{Acm}^{-2}$ to $0.03 \mu\text{Acm}^{-2}$ with a short change of potential of 0.087 V after which the current density increases to $0.033 \mu\text{Acm}^{-2}$ when the potential increases from 0.087 V to 0.146 V . The current density is then observed to decrease from $0.036 \mu\text{Acm}^{-2}$ to $0.031 \mu\text{Acm}^{-2}$ when the generated voltage increases from 0.188 V to 0.26 V .

It was observed that after a potential of 0.221 V , there was an exponential decrease in current up to a potential of 0.259 V where the observed current was $0.001 \mu\text{Acm}^{-2}$. However, cell T¹ had characteristic curve deviation from that of an ideal cell was attributed to the varying constituent from the expected optimized values. A solar cell works well when the conductance is infinite (Galymzhan, 2010). The effect of decrease in current between a potential of 0 V to 0.087 V is attributed to the shunt resistance in the cell. Increase in voltage between a potential of 0.146 V to 0.26 V has a very small variation in current of $0.003 \mu\text{Acm}^{-2}$ since the curve takes a constant profile. This can be attributed the charge carriers encountering a region of almost uniform cell resistance (Imran, 2013). Further experiments were carried out with cells made of different ratios as discussed in the next section.

Analysis of cell U¹

The effect of resistance of cell U¹ with composition of TiO_2 (0.7 g), graphite (0.25 g) and iodine (0.18 g) was investigated as presented in Table 5.

Table 5: Composition of materials in cell U¹

| U ¹ | Mass (g) | | | |
|----------------|------------------|------|----------|----------------|
| | TiO ₂ | KI | Graphite | I ₂ |
| | 0.7 | 0.01 | 0.25 | 0.18 |

The resulting current density against each corresponding value of potential was recorded as shown in Table 5.

Table 5: Generated potential against current density of cell U¹

| Output cell parameters | |
|------------------------|--|
| Voltage (V) | Current (J _{sc} (μAcm^{-2})) |
| 0 | 0.022 |
| 0.079 | 0.026 |
| 0.147 | 0.022 |
| 0.189 | 0.024 |
| 0.204 | 0.023 |
| 0.228 | 0.023 |
| 0.235 | 0.021 |
| 0.242 | 0 |

From the information recorded in of potentials against the current Figure 3 below.

Table 5, a graphical representation density was made as shown in

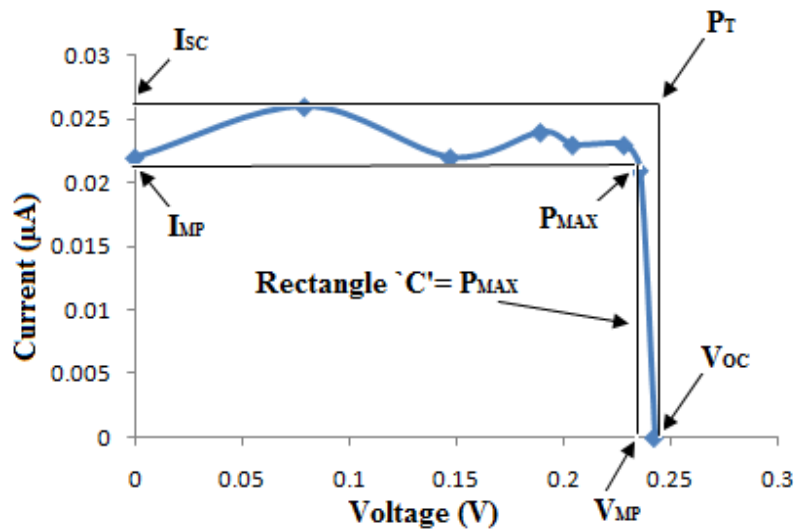


Figure 3: I-V characteristics of cell U¹

From Figure 3, a gradual increase in current density was observed from 0.024 μAcm^{-2} with little variation 0.002 μAcm^{-2} between a voltage of 0.079 V and 0.147 V. This I-V characteristics curve is almost uniform with very little variation. The series resistance between a potential of 0.230 mV to 0.235 mV increased to 4.17 Ω . This can be attributed to the ratio of the electronegative

constituent to be above the adequate level that replenishes the deficiency created when electrons are excited from the photo active material hence generating very little current density (Imran, 2013).

However, S^1 , T^1 and U^1 did not exhibit the properties of an ohmic conductor, since cells S^1 and T^1 had an initial current density of about $0.05 \mu\text{Acm}^{-2}$ while cell U^1 had an initial current density of $0.026 \mu\text{Acm}^{-2}$. The difference could be attributed to the content of TiO_2 which was the determinant of the charged species, and therefore current was proportional to the quantity of this material. However, these results obtained showed that in these type of cells, the generated potential was affected by many factors. These cells did not exhibit the properties of ohmic conductors. A similar observation was reported by Scott (2009) as he characterized TiO_2 dye sensitized cells. Maximum power output can be obtained from the characteristic curves by constructing the largest rectangle under the curve. Maximum current density and voltage were obtained from their X and Y axes respectively, formed by their respective rectangles.

Fill Factor, Efficiency, Series and Shunt Resistance of Cell S^1 , T^1 and U^1

A summary of Fill Factor, efficiency, series and shunt resistance of cell S^1 , T^1 and U^1 is as presented in Table 6.

Table 6: Summary of optimal parameters of cells S^1 , T^1 and U^1

| Cell | FF | $\eta\%$ | Series Resistance (R_s) Ω | Shunt Resistance ($R_{SH}\Omega^{-1}$) |
|-------|------|----------|--------------------------------------|--|
| S^1 | 0.58 | 5E-6 | 8.65 | 0.116 |
| T^1 | 0.49 | 4E-6 | 4.255 | 0.235 |
| U^1 | 0.76 | 3E-6 | 4.167 | 0.24 |

Parameters of Cells with Different Thickness

A comparison of the parameters obtained from the three cells with different thickness was analysed and presented in Table 7. The parameters compared are, current density, open circuit voltage, fill factor and the efficiency of cells S^1 , T^1 and U^1 . The results are similar to the ones observed by (Kavita, 2011).

Table 7: Comparison of J_{SC} , V_{OC} , FF and η % of cells S^1 , T^1 and U^1

| Sample | $J_{SC}(\mu\text{A}/\text{cm}^2)$ | $V_{OC}(\text{V})$ | FF | $\eta\%$ |
|--------|-----------------------------------|--------------------|------|----------|
| S^1 | 0.046 | 0.222 | 0.37 | 4E-6 |
| T^1 | 0.033 | 0.199 | 0.35 | 2E-6 |
| U^1 | 0.025 | 0.132 | 0.56 | 1E-6 |

Another factor that affected the performance of the solar is the internal resistance due to the parallel layers of the cell constituent materials. These layers form a region of dielectric which slow down the migration of charge carriers due to capacitive effect of the dielectric material. A

similar scenario was reported by (Imran, 2013). Imran attributed the capacitance due to the double layer and presented that scenario in a pictorial scheme as presented in Figure 4.

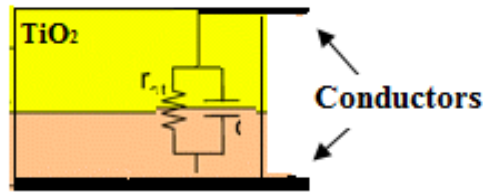


Figure 4: Sketch of the cell with resistance and capacitance opposing charge carriers migration

Source: Imran (2013)

The Optimized Cell Performance

Having considered the mass ratios of the optimized cell V^1 with TiO_2 (0.4 g), C_X (0.3 g) and I_2 (0.17 g) constituent materials which generated the highest potential as presented in Table 8, and the optimized thickness, the effect of protective adhesive glue was investigated and the data obtained is presented in Table 9.

Table 8: Optimal Mass (g) values used to fabricate the optimized solar cell V^1

| V^1 | Mass (g) | | | |
|-------|----------|------|----------|-------|
| | TiO_2 | KI | Graphite | I_2 |
| | 0.4 | 0.01 | 0.30 | 0.17 |

The analysis of the resulting potential and current was done on different optimized cells with (1, 2, 3, 4 and 5) grid conductors, void and with protective adhesive glue. The generated potential and current against the corresponding number of conductors on the grid was monitored and the results obtained are as presented in Table 9.

Table 9: Generated potential and current of the optimized cells with and void of adhesive protective glue

| No of grid conductors on each cell | Potential (V) and Current (μAcm^{-2}) | | | |
|------------------------------------|--|----------------------------|-------------------------|----------------------------|
| | Cell Void of adhesive glue | | Cell with adhesive glue | |
| | Potential(V) | Current (μAcm^{-2}) | Potential (V) | Current (μAcm^{-2}) |
| 1 | 0.337 | 1.96 | 0.240 | 0.26 |
| 2 | 0.470 | 2.49 | 0.402 | 0.54 |
| 3 | 0.56 | 3.54 | 0.509 | 1.53 |
| 4 | 0.754 | 5.15 | 0.682 | 2.62 |
| 5 | 0.803 | 5.82 | 0.724 | 3.11 |

From the information recorded in Table 9, a graphical presentation of potentials against the number of conductors on the grid was made as presented in Figure 5.

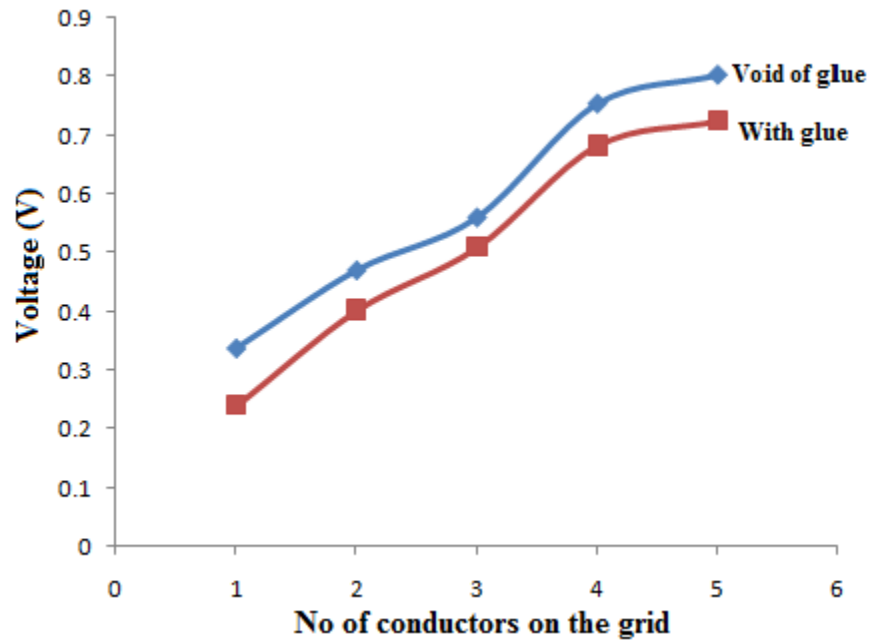


Figure 5: Characteristic curve of potential against varied conductors grid of cells with and void of protective glue

It shows that the cells void of protective adhesive glue had higher potential as opposed to the cells with protective glue. This could be attributed to the adhesive glue absorbed some of the radiation resulting to a lesser number of excited charge carriers. However, it was also observed that the more the number of conductors on the grid the more the potential. This could be attributed to the grid enhancing collection of more charge carriers at the surface of the cell.

A graphical presentation of the resulting current density against the number of conductors on the grid of cells void and with protective adhesive glue, was made as shown in Figure 6 using the results presented in Table 9.

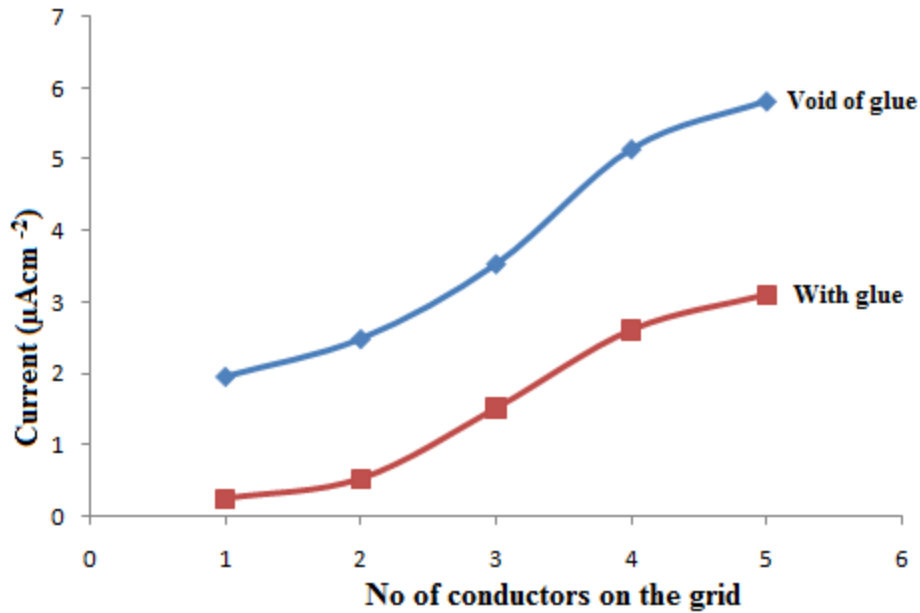


Figure 6: Characteristic curve of current against varied conductors grid of cells with and void of protective glue

Similar profiles were observed confirming that the protective glue was the one responsible for the resulting amount of potential and current. This shows that even if the protective glue was preferred to enhance compatibility of the solar cell, there has to be agreement on the transparent conducting oxides instead of the glue and the conducting grid to enable penetration of the photo energy and migration of charge carriers.

I-V Characteristic of the Optimized Solar Cell

Having established the optimum ratios and the factors that contributed to deriving the best results, a solar cell void of protective glue was fabricated with TiO₂ (0.4 g), C_X (0.3 g) and I₂ (0.17 g) constituent materials as presented in Table 8.

Table 8: Optimal Mass (g) values used to fabricate the optimized solar cell

| V ¹ | Mass (g) | | | |
|----------------|------------------|------|----------|----------------|
| | TiO ₂ | KI | Graphite | I ₂ |
| | 0.4 | 0.01 | 0.30 | 0.17 |

The cell was then characterized and the generated current against the potential are as recorded in Table 9.

Table 9: Generated potential against current density of the optimized cell

| Output cell parameters | |
|------------------------|--|
| Voltage (V) | Current density ($J_{\mu Acm^{-2}}$) |
| 0 | 12.037 |
| 0.448 | 11.469 |
| 0.681 | 10.684 |
| 0.793 | 9.423 |
| 0.879 | 7.534 |
| 0.951 | 3.985 |
| 0.958 | 3.257 |
| 0.961 | 2.966 |
| 0.964 | 2.831 |
| 0.97 | 1.571 |
| 0.979 | 0.0141 |

From the information recorded in Table 9, a graphical representation of the current density against the potentials generated was made as shown in Figure 7.

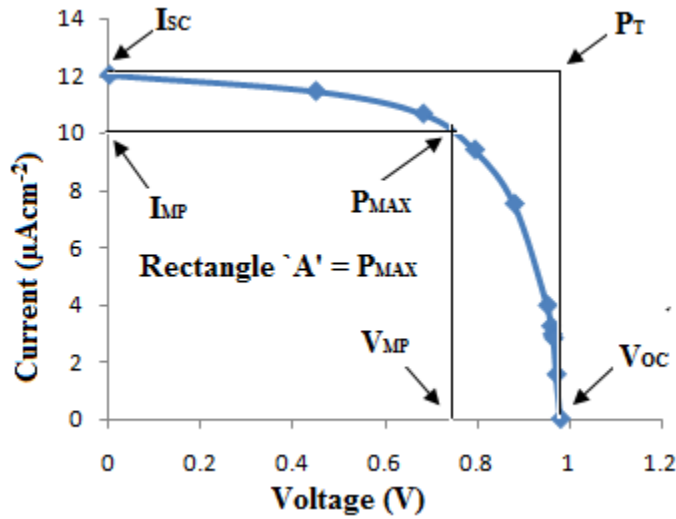


Figure 7: Characteristic curve of current density against the potential of the optimized cell

The I-V curve of the cell with the optimized parameters resembles that reported by Imran (2013) as he studied the power (P_{MAX}) of a photo cell. The results show a normal I-V curve profile with decrease in current as the potential increases. It can be seen from the graph of figure 4.19 that a maximum current density of $12.037 \mu A/cm^2$ was recorded at a potential of 0 V. However, a maximum potential of 0.979V was observed when the current reduced to $0.0141 \mu Acm^{-2}$.

The finding is in agreement with other similar studies (Imran, 2013). From this information, the maximum power produced by the cell was calculated taking into consideration the area and the maximum power rectangle as reported by (Imran, 2013).

The parameters – Maximum Voltage (V_{MP}) , Maximum current density (J_{MP}), short circuit current density (J_{SC}/cm^2), maximum power(P_{MAX}), P_T , fill factor (FF) and the conversion

efficiency (η %) – were determined as presented in Table 10 which presents a summary of cell V^1 , S^1 , T^1 and U^1 performance characteristics.

Table 10: Comparison of J_{SC} , V_{OC} , FF and $\eta\%$ of cells V^1 , S^1 , T^1 and U^1

| Sample | $J_{SC}(\mu A/cm^2)$ | $V_{OC}(V)$ | FF | $\eta\%$ |
|--------|----------------------|-------------|-------|----------|
| V^1 | 12.037 | 0.979 | 0.641 | 0.006 |
| S^1 | 0.046 | 0.222 | 0.37 | 4E-6 |
| T^1 | 0.033 | 0.199 | 0.35 | 2E-6 |
| U^1 | 0.025 | 0.132 | 0.56 | 1E-6 |

The maximum Voltage (V_{MP}) and maximum current density (J_{MP}) of this cell were obtained as 0.754 V and $10.013 \mu A/cm^2$ for a P_{MAX} of $7.5 \mu W$ and a P_T of $11.784 \mu W$. It was observed that the optimized cell yielded efficiency (η) of 0.006% and a fill factor (FF) of 0.641. Thicker layers of TiO_2 limit penetration of radiation in the photo active electrode thus limiting the light harvesting ability of the solar cells (Martin, 2012). Maximum power output was obtained for the other S^1 , T^1 and U^1 cells where the V_{oc} had very small deviation but the current was found to vary with a bigger margin depending on the constituent of the cell materials. The varied amount of the current generated was suggested to be contributed by the internal resistance of the composition of each cell (Potsavage, 2011).

Despite graphite being the conduit for the migration of electrons, too much of it contributed to thicker layers of the cell as observed in cell U^1 with mass ratio (0.7: 0.25: 0.18) of TiO_2 : graphite: I_2 . This contributed to poor penetration of radiation, hence low energy to activate the photo conducting material. Interfaces between the two cell layers caused contact resistance which contributed to reduction of the cell efficiency resulting to inefficient charge carrier migration (Coakley *et al.*, 2005).

This study also found out that varied cell composition resulted to internal cell impedance. On observing the characteristic curves of cells S^1 , T^1 and U^1 , the initial current at zero potential was high but decreased with increase in potential. Further observation on the cells, lead to the conclusion that the cell mass composition had effects on the output, since the optimized cell V^1 had the best efficiency of 0.006%.

The results presented in Tables 10 and 11 confirm that cell V^1 with optimized parameters yielded the highest current density of $12.037 \mu A/cm^2$, potential of 0.979 V and an efficiency of 0.006% with a Fill Factor of 0.641. Table 11 further compares the parameters P_{MAX} , P_T and V_{MP} calculated during the analysis of the four cells with different thicknesses.

Table 11: Summary of P_{MAX} , P_T and V_{MP} parameters of cells V^1 , S^1 , T^1 and U^1

| Cell | $V_{OC}(V/cm^2)$ | $J_{SC}(\mu A/cm^2)$ | $V_{MP}(V/cm^2)$ | $J_{MP}(\mu A/cm^2)$ | $P_{MAX}(\mu W)$ | $P_T(\mu W)$ | FF | $\eta\%$ |
|-------|------------------|----------------------|------------------|----------------------|------------------|--------------|-------|----------|
| V^1 | 0.979 | 12.037 | 0.754 | 10.013 | 7.550 | 11.784 | 0.641 | 0.006 |
| S^1 | 0.248 | 0.050 | 0.200 | 0.037 | 0.007 | 0.012 | 0.590 | 0.005 |
| T^1 | 0.259 | 0.048 | 0.210 | 0.028 | 0.006 | 0.012 | 0.473 | 0.004 |
| U^1 | 0.242 | 0.024 | 0.24 | 0.021 | 0.005 | 0.006 | 0.867 | 0.004 |

CONCLUSION

A solar cell was successfully fabricated using TiO_2 which is a nontoxic, chemically inert and stable material. The resulting cell was characterized in clear day light. The variation of current generated against its corresponding potential for the various cells was collected and the results obtained indicated that there is potential in the development of the photocell using TiO_2 graphite and I_2 materials in the mass ratios (0.4: 0.3: 0.17) for application at the point of use. These ratios yielded the best results of ($V_{OC} = 0.979\text{V}$, and $J_{SC} = 12.037\mu\text{Acm}^{-2}$, $P_{MAX} = 7.55\mu\text{W}$, fill factor (FF) = 0.64 and efficiency (η) = 0.006%).

The general trend observed was that increase in the ratio of the photo active material generated higher potential which drastically reduced after the optimized ratio was reached, and the generation of potential reduced considerably. Considerable potential was generated with some ratio of iodine-iodide complex indicating that its presence contributed to generation and subsequent increase in voltage. The highest potential (V_{OC}) of 0.956V was generated with I_2 mass of 0.15 g. Certain thickness of the photo active material (TiO_2) and graphite (C_X) were observed to affect the cells output since variation of TiO_2 generated varied potentials. A thickness of 2 mm and 1 mm of TiO_2 and graphite respectively yielded the highest potential of 0.979 V. This lead the researcher to the conclusion that thickness affects penetration of radiation and also increases the parasitic resistance to the migrating electrons.

In all the cells characterized, even at constant radiation illumination, the V_{oc} was constant but current differed with a factor that could have been contributed by the internal resistance. From the results obtained on optimization of a blank cell, the open circuit voltage (V_{OC}) and short circuit current density (J_{SC}) of 0.083 V and $0.33\mu\text{A}$ were respectively obtained. These values were low confirming that a conducting medium was necessary for the migration of the generated electrons.

REFERENCES

- Adegbenro, A. (2016). *Comparison of novel and state of the art solar cells*. University of Kessel, Germany.
- Coakley, K. M., Liu, Y., Goh, C., & McGehee, M. D. (2005). Ordered organic-inorganic bulk heterojunction photovoltaic cells. *Cambridge University Press bulletin MRS*, 37-40.
- Ferguson, R., Wilkonson, W., & Hil, R. (2000). *Electricity Use and Economic Development*, 28. Energy Policy. Florida, USA.
- Fungo, F. (2007). *Photosensitization of Nanocrystalline Semiconductor Film electrodes*. New Jersey: Prentice-Hall, Inc.
- Galymzhan, T. K. (2010). *Analysis of Impact of non-uniformities on Thin-film Solar Cells and Modules with 2-d simulations*. Colorado State University Fort Collins, Colorado.
- Hagfeldt, A. G., Boschloo, L. S., Kloo, L., & Pettersson, H. (2010). Dye-Sensitized Solar cells. *Catalysis*, 110, 6595-6663.
- Imran, K. (2013). *A Study on the Optimization of Dye-Sensitized Solar Cells* (PhD Thesis). University of South Florida.

- IPCC (2006). *Guidelines for National Greenhouse Gas Inventories Technical report*. Inter-Governmental Panel on Climatic Change. Hershey: Information Science Reference.
- Kavita, S. (2011). *Comparing Morphological Properties and Conduction Phenomena in Si Quantum Dot Single Layers and Multilayers*. Francais: University of Grenoble.
- King, D., Hansen, B., Kratochvil, J., & Quintana, M. (1997). Dark current voltage measurement on photovoltaic module as a diagnostic or manufacturing tool. In *the proceedings of the 26th IEEE Photovoltaic Specialized Conference*, 26, pp. 1125-1128. Anaheim: California.
- Ohama, Y., & Van, G. (2011). *Pre-irradiation of anatase TiO₂ particles with UV enhances electron-holes activation*. Journal of hazardous materials, 196, 145-152. Retrieved January 10, 2017 from <https://doi.org/10.1016/j.jhazmat>
- Piliouguine, M. Carretero, J. Mora-lopez, L. & Sidrach-de-cardona, M. (2011). Experimental system for current-voltage curve measurement of photovoltaic modules under outdoor conditions. *Progress in Photovoltaic Research and Application*, 19(5), 591-598.
- Potsavage, (2011). Physics and Engineering of Organic Solar Cells *Journal of Physical Chemistry Letters*, 2(15), 1950-1964.
- Renu, G. Amit, J. & Avinashi, K. (2012). *Exact Analytical Analysis of Dye Sensitized Solar Cell: Improved Method and Comparative Study*, Delhi University, New Delhi, India.
- Scott, B. (2009). *The Fabrication and Characterization of Organic Solar Cells* (Unpublished thesis). Texas University, Austin.
- Sellappan, R. (2013). *Mechanisms of Enhanced Activity of Model TiO₂/Carbon and TiO₂/Metal Nanocomposite Photocatalysts*. University of Technology.
- Yordanov, G. H. (2012). *Characterization and Analysis of Photovoltaic Modules and the Solar Resource Based on In-Situ Measurements*. Norwegian University Southern Norway.